AEROSOL REMOTE SENSING WITH AATSR: A DUAL-VIEW SURFACE BRDF OPTIMAL ESTIMATION RETRIEVAL SCHEME

A. M. Sayer[1], R. G. Grainger[1], C. T. Mutlow[2], G. E. Thomas[1]

1. Atmospheric, Oceanic and Planetary Physics, Department of Physics, University of Oxford
2. Rutherford Appleton Laboratory, Chilton, Didcot, Oxfordshire

sayer@atm.ox.ac.uk

ABSTRACT

The differing path lengths of AATSR's forward and nadir views are used to separate the contributions from aerosol scattering and surface reflectance in the observed top-of-atmosphere (TOA) radiance. This poster presents an extension of the Oxford-RAL retrieval of Aerosols and Clouds (ORAC) scheme used by the GRAPE and GlobAEROSOL projects (Thomas *et al.*, 2007), which currently uses vis/nIR data from the nadir viewing geometry only, to take advantage of the dual-view capabilities AATSR offers. Additionally, a surface bidirectional reflectance distribution function (BRDF) forward model has been implemented to replace the previous Lambertian assumption.

The new algorithm uses optimal estimation to retrieve aerosol optical depth at 550 nm, effective radius and the effective Lambertian surface albedo at 550 nm (with the spectral shape of the surface constrained by a model based on Cox and Munk (1954a,b) statistics for sea, and MODIS BRDF data (Wanner *et al.*, 1997) for land).

INSTRUMENTAL DETAILS

The Advanced Along-Track Scanning Radiometer (AATSR) aboard Envisat (launched March 2002) is the successor of the earlier similar instruments ATSR and ATSR-2. It measures TOA reflectance at 7 wavelengths in the visible and IR, four of which (550 nm, 660 nm, 870 nm and 1.6 μm) are used in the aerosol retrieval.

A special feature of the instruments is their two viewing geometries. They obtain forward-view measurements at a zenith angle of 53°-55°, and around 100 seconds later sample the same region at a nadir viewing zenith angle of 0°-22°.

The swath width is 512 km allowing global coverage every 3 days. Ground pixel resolution is approximately 1 km by 1 km for the nadir view and 1.5 km by 1.5 km for the forward; as a result the retrieval is normally performed at 3 km by 3 km resolution. This 'superpixelling' to a lower resolution additionally decreases the effect of instrumental noise.

RETRIEVAL ALGORITHM

ORAC is an optimal estimation (OE) retrieval (Rodgers, 2000) employing Levenburg-Marquadt iteration to find a solution. The rigorous statistical basis of the OE scheme provides the following advantages:

1. Estimates of error on retrieved parameters
2. Quality control on the solution (retrieval 'cost')
3. Assimilation of *a priori* information on the surface and atmospheric state

Satellite input is a total of 8 measurements of TOA reflectance (4 channels at two geometries). From this the aerosol optical depth τ (Equation 1) at 550 nm, distribution effective radius r_e (Equation 2) and effective Lambertian surface albedo at 550 nm are retrieved.

$$\tau(\lambda) = \int_0^\infty \beta_e(z,\lambda)\,dz$$

Equation 1: Aerosol optical depth

$$r_e = \frac{\int_0^\infty r^3 n(r)\,dr}{\int_0^\infty r^2 n(r)\,dr}$$

Equation 2: Effective radius

AEROSOL MODEL

Aerosol microphysical properties from the OPAC database (Hess *et al.*, 1998) have been used to generate aerosol class models corresponding to typical biomass burning, continental, maritime, dust and urban aerosol. Each class consists of up to 4 aerosol components, represented by lognormal distributions with differing modal radius and spread. Size distributions with different effective radii are obtained by altering the mixing ratio of these components. These models are then fed into the atmospheric forward model.

ATMOSPHERIC FORWARD MODEL

The purpose of the forward model is to predict TOA radiance given atmospheric and surface conditions. The aerosol class models are used with the DISORT radiative transfer code (Stamnes *et al.*, 1988) and MODTRAN gas absorption database (Brown *et al.*, 2004) to generate lookup tables (LUTs) of atmospheric transmission and reflectance over a range of geometric and aerosol conditions. Additionally, three different surface reflectances are defined:

1. The bidirectional reflectance of the surface, R_{YBD}. This makes use of *a priori* information dependent on the pixel type, and is defined by a BRDF. Land pixels use the MODIS land surface BRDF product (Wanner *et al.*, 1997), while over the ocean a model based on Cox and Munk (1954a,b) wave statistics is employed. This term depends on solar and viewing angles.

2. The black-sky albedo, R_{YB}. This is obtained by integration of the bidirectional reflectance over all satellite zenith and relative azimuth angles, and hence only depends on solar angle. It represents the scattering of a direct beam of light over a hemisphere.

3. The white-sky albedo, R_{YW}. This is obtained by integration of the black-sky albedo over all solar angles, and hence has no geometric dependence. It is also known as the effective Lambertian albedo. The retrieved surface product is a white-sky albedo.
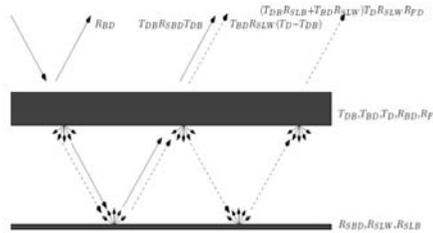

Figure 1: Surface-atmosphere interactions in the forward model (image courtesy Gareth Thomas)

Multiple scattering between the surface and atmosphere as shown in Figure 1 is used to predict the TOA reflectance according to Equation 3. The R_X and T_X are the reflectance or transmittance of the atmosphere to direct and diffuse radiation, and are functions of geometry and aerosol properties.

$$R = R_{BD} + T_{DB}\left(R_{SBD} - R_{SB}\right)T_{DB} + \frac{\left(T_{DB}R_{SB} + T_{BD}R_{SW}\right)T_D}{1 - R_{SW}R_{FD}}$$

Equation 3: TOA reflectance

During the retrieval, the spectral shape of the surface is fixed. The absolute magnitude of the white-sky albedo at 550 nm is allowed to vary, with the black-sky and bidirectional reflectance at 550 nm scaled by the same amount (assuming that a small change in one term has a linear impact on the others). Reflectances at the other wavelengths are then adjusted to retain the spectral shape.

ITERATION AND QUALITY CONTROL

Starting from a first guess at the atmospheric state x, set equal to the a *priori* values x_b, linear interpolation of the LUTs is used to give a first estimate of TOA reflectance. This is compared to the observed values y_m and iteration proceeds via a weighted combination of steepest descent and Newtonian steps (the Levenburg-Marquadt method). The solution is found based on the minimisation of a cost function, J (Equation 4). This is a least-squares fit of the measurements, weighted by the uncertainty on them (S_y) and *a priori* values (S_x). Up to 25 iterations are permitted before iteration is abandoned; failure to converge is noted.

$$J = \left(y(x) - y_m\right)S_y^{-1}\left(y(x) - y_m\right)^T + \left(x - x_b\right)S_x^{-1}\left(x - x_b\right)^T$$

Equation 4: The cost function

The retrieval is not performed in cases of cloud cover. A simple radiance ratio test is applied to the data before iteration to flag clouds, using both viewing geometries.

SAMPLE RESULTS

A comparative study with other satellite and AERONET data over continental Europe has been performed (Kokhanovsky *et al.*, 2007) using data from the Lambertian ORAC retrieval for October 13th 2005. A false-colour image of the region is shown in Figure 2.
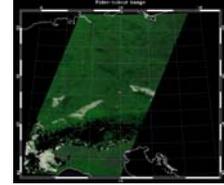

AATSR optical depth retrievals were found to have a positive bias as compared to the other sensors. Development of the dual-view BRDF algorithm has enabled a reprocessing of the scene in question and comparisons to the nadir-view Lambertian retrieval as used in the GRAPE project.

Figure 2: False-colour image of the scene discussed in Kokhanovsky *et al.* (2007)
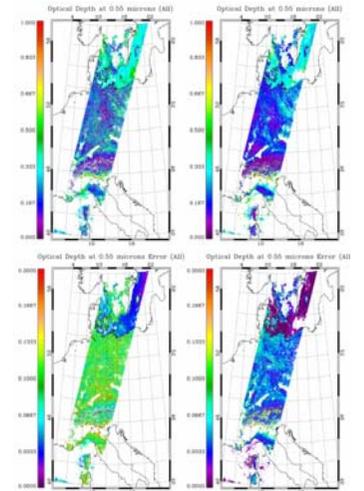

Figure 3: Retrieved aerosol optical depth at 550 nm (top) and associated error estimates (bottom) for the nadir-view Lambertian model (left) and new dual-view BRDF model (right).
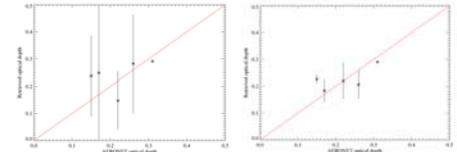

Figure 4: Comparison of retrieved aerosol optical depth at 550 nm with ground-based data. Results shown for the nadir-view Lambertian model (left) and dual-view BRDF model (right). Satellite values are the mean of a 0.1° box around the ground station with error bars indicating the variability of this box.

Figures 3 and 4 show that implementation of the dual-view BRDF has resulted in generally slightly lower optical depths, and a much reduced scatter in the retrieved field. The trend in the ground-based data is better captured. These are encouraging results, particularly considering the general positive bias of AATSR observed in Kokhanovsky *et al.* (2007). Error estimates are considerably smaller.

The correlation coefficient for the Lambertian data in Figure 4 is 0.41 and that for the BRDF data is 0.68. The measurement at Hamburg (showing the lowest AERONET optical depth, 0.17) lies outside the AATSR swath, but corners of the 0.1° box fall within the swath. It is therefore not surprising that agreement is poorest for this station. If it is neglected, correlation coefficients become 0.49 for the Lambertian retrieval and 0.88 for the BRDF.

AERONET and the University of Bremen are thanked for the ground-based data.

CONCLUSIONS

The dual-view BRDF retrieval offers several key improvements over the standard nadir-view ORAC retrieval.

• Smoother retrieved aerosol profiles

• Improved agreement with ground-based data

• Smaller error estimates on retrieved quantities

• Better cloud flagging, as both views may be used

FUTURE WORK

1. Incorporate the IR channels into the retrieval scheme. This will improve characterisation of effective radius, as well as allow retrieval of aerosol layer height and surface temperature.

2. Improve the sea surface reflectance model to include the effect of absorption of light by coloured dissolved organic matter (CDOM)—expected to be important at 550 nm.

3. Continue to validate against ground-based and other satellite data products.

REFERENCES

J. Brown, M. Hoke, K. Doherty, G. Anderson, A. Berk, MODTRAN 4 software, 2004, *http://www.vs.afrl.af.mil/ProductLines/IRClutter/modtran4.aspx*

C.S. Cox, W.H. Munk, Measurement of the roughness of the sea surface from photographs of the Sun's glitter, *J. Opt. Soc. Am.*, 1954a, **44**, 838-850.

C.S. Cox, W.H. Munk, Statistics of the sea surface derived from Sun glitter, *J. Mar. Res.*, 1954b, **13**, 198-227.

M. Hess, P. Koepke, I. Schult, Optical properties of aerosols and clouds: The software package OPAC, *Bull. Am. Met. Soc.*, 1998, **79**(5), 831-944.

A.A. Kokhanovsky, F-M. Breon, A. Cacciari, E. Carboni, D. Diner, W. Di Nicolantonio, R.G. Grainger, W.M.F. Grey, R. Höller, K-H. Lee, Z. Li, P.R.J. North, A. Sayer, G. Thomas, W. von Hoyningen-Huene, Aerosol remote sensing over land: a comparison of satellite retrievals using different algorithms and instruments, *Atmos. Res.*, 2007, in press.

C.D. Rodgers, Inverse methods for atmospheric sounding: Theory and Practice, 2000, *World Scientific*.

K. Stamnes, S-C. Tsay, W. Wiscombe, K. Jayaweera, Numerically stable algorithm for discrete-ordinate-method radiative transfer in multiple scattering and emitting layer media, *Appl. Opt.*, 1988, **27**(12), 2502-2509.

G.E. Thomas, S.H. Marsh, S.M.Dean, E.Carboni, R.G.Grainger, C.A.Poulsen, R.Siddans, B.J. Kerridge, An optimal estimation retrieval scheme for (A)ATSR, *AOPP Memorandum 2007.1*, 2007.

W. Wanner, A.H. Strahler, B. Hu, P. Lewis, J-P. Muller, X. Li, K. Schaaf, C.L. Barker, M.J. Barnsley, Global retrieval of bidirectional reflectance and albedo over land from EOS MODIS and MISR data: Theory and algorithm, *J. Geophys. Res.*, 1997.